

## Preliminary geoelectrical identification of a low-temperature hydrothermal system in the Anzer glacial valley, İkizdere, Rize, Turkey

Abdullah KARAMAN\*

Istanbul Technical University, Department of Geophysics, Maslak 34469, İstanbul, Turkey

Received: 18.07.2012 • Accepted: 13.11.2012 • Published Online: 13.06.2013 • Printed: 12.07.2013

**Abstract:** The Anzer glacial valley, at an elevation of over 2300 m in the Eastern Black Sea region of Turkey, exhibits evidence for a low-temperature hydrothermal system (40–100 °C). Low-temperature hydrothermal systems usually do not receive attention since they are not useful for energy production. However, in areas where natural beauty is prominent, as in the Anzer valley, such resources can easily trigger investment for all-season resorts that significantly contribute to the economy. In this study, we examine the site evidence and carry out self-potential and dc-resistivity sounding surveys using a Schlumberger electrode configuration. The resistivity cross-section obtained from the inversion of a number of 1-D Schlumberger soundings, integrated with the slopes obtained from the inversion of the self-potential anomalies, suggests a conductive zone corresponding to the mineral alteration zone surrounding the crack conduits in this hydrothermal system. This study also emphasizes the significance of low-temperature hydrothermal fields for the region.

**Key words:** Geothermal, hydrothermal, self-potential, dc-resistivity, Rize, İkizdere, Anzer, Ballı, Black Sea

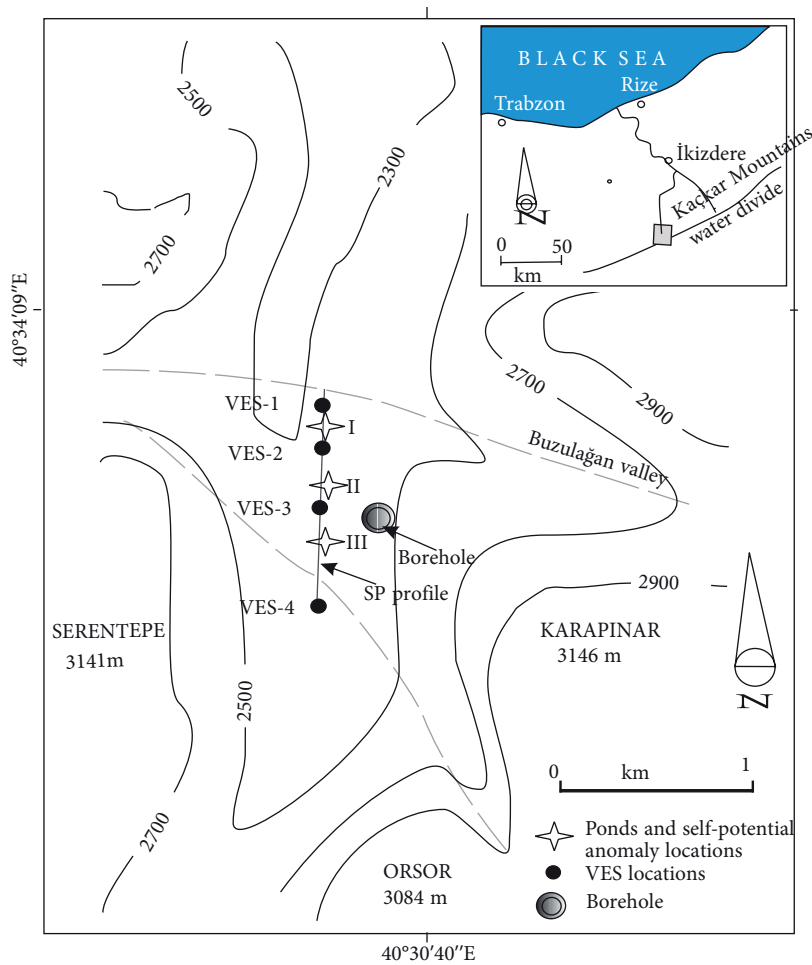
### 1. Introduction

Figure 1 shows the location of the Anzer glacial valley, which is at over 2300 m altitude. This rugged part of Turkey, inland from the Black Sea, includes forested steep mountainsides separated by valleys, with areas of high pasture. Ballı village, at the terminus of the Anzer valley, is one of several remote villages on the northern flank of the Kaçkar Mountains. The valley appears to have potential for all-season sports and recreation since it is unique with its extremely rich flora, growing from the spring to autumn (Ozkırım & Keskin 2001; Doğan & Kolankaya 2005). However, the valley and the village have to be evacuated in winter since the living conditions become very harsh and the access roads become difficult to maintain. Recently, reports from the local people about gas bubbles and occasional vapor exhalation from the ponds in a number of locations in the valley motivated us to investigate the site's hydrothermal potential with the hope of opening up new opportunities for the local economy by triggering new investments that may eventually yield an increase in tourism revenue. Geothermal studies in this part of the country are rare, to the best of our knowledge, and this study may lead to new public surveys and exploration programs for new fields.

Hydrothermal field exploration requires a clear understanding of the hydrothermal activities that are

related to a particular hydrothermal system (Pirajno 1992). Hydrothermal alteration, bacterial colonies, soil and water temperatures, and other field evidence require careful inspection. A good resistivity contrast, such as occurs between fractured and compact crystalline rocks, imposes marked resistivity anomalies on the resistivity profiles (Majumdar *et al.* 2000). We therefore carried out dc-electrical measurements with a Schlumberger electrode configuration and self-potential measurements to identify possible crack systems and fault zones leading to the hot water upwelling and emerging in the form of a warm pool. Dc-electrical and self-potential methods have been successfully used in identifying common shallow features such as faults, fracture systems, and alteration zones encountered in hydrothermal sites (e.g., Ogilvy *et al.* 1969; Bogoslovsky & Ogilvy 1973; Harthill 1978; Mabey *et al.* 1978; Tripp *et al.* 1978; Ward *et al.* 1978; Corwin & Hoover 1979; Fitterman & Corwin 1982; Murakami *et al.* 1984; Zohdy & Bisdorf 1990; Pirajno 1992; Majumdar *et al.* 2000; Storz *et al.* 2000; Reci *et al.* 2001). Harinarayana *et al.* (2006) and Spichak (2009) utilized magnetotelluric and electromagnetic sounding measurements at greater exploration depth to obtain the resistivity structure of geothermal fields. This present study utilizes conventional geophysical methods to identify the crack system/fault zone. However, the real value of this study is to motivate

\* Correspondence: karaman@itu.edu.tr



**Figure 1.** The location of the study site (inset figure). The contour lines show the elevations in meters above mean sea level. The thick dashed lines show the major crack zones mostly separating the peaks and crests in the area.

other exploration programs in the rarely studied Eastern Black Sea Region of Turkey, and, ultimately, to create an economic impact.

## 2. Site description

The geology of the Kaçkar Mountains is described extensively by Okay and Şahintürk (1997) and Şengör and Yılmaz (1981). The site, as shown in Figure 1, is located on the northern side of the Eastern Black Sea Mountains where an E-W trending belt consists mostly of magmatic rocks. This magmatic belt is an east-west trending continental margin arc developed in response to the northward subduction of the northern branch of oceanic crust beneath the Eurasian plate. Magmatic activity in the area began in the Turonian and continued until the end of the Paleocene. During the same period, granitic intrusions were emplaced into shallow levels of the crust and formed the first components of a composite pluton called the Rize

granite. Emplacement of the pluton occurred in pulses and lasted until the late Eocene. Bounded to the south by the watershed, the Anzer valley is about 20 km long and a few hundred meters wide, and receives heavy snow. Lateral moraines at the sides of the valley appear to be replaced with outwash deposits just outside Ballı village, forming flat-land for the settlement.

Figure 1 illustrates two major crack systems that we were able to identify from the rock outcrops at the sides of the valley; one intercepts the valley in an east-west direction and the other is about 30° oblique to the valley's axis. The warm pools that are strictly bounded with these major crack systems exhibit hematitization and iron-rich alteration at their outlets. Hematitization related to hydrothermal alteration is not well documented, since it is usually associated with late-stage (therefore, low-temperature) hydrothermal activity (Pirajno 1992). No further evidence for warm water was found outside this

triangular zone that is about 1 km long along the axis of the Anzer valley.

Intermittent gas bubbles (fumaroles) in small ponds with tiny cracks or holes at the bottom were observed at a number of places. The ponds observed between the two major crack systems may have formed after the removal of top soil particles dislodged by gas emerging at the Earth's surface, like pockmarks that occur in seabed sediments from gas eruptions. The water temperature measurements in a number of these ponds showed a maximum temperature of 23 °C in near-freezing air while the mean surface water temperature was about 5-7 °C. Such an anomalous water temperature in these ponds maintains a favorable environment for fungus, bacterial colonies, frogs, and insects, when the air temperature drops below 0° and permafrost reaches to a depth of about 1 m on land at such elevations. Because the side walls of the valley were mostly covered with a thick angular lateral moraine, we were unable to align geophysical measurements perpendicular to the valley axis. The bottom of the valley, being a gently rolling pasture, allowed us to obtain only 1-D geophysical measurements.

**3. Data acquisition and interpretation**

To characterize the crack systems and determine the effect of the fractured zones acting as conduits, we carried out vertical electric soundings at four locations (Figure 1) using the Schlumberger electrode configuration. The electrodes were spread along N-S directions, with the center of the array marked as VES-x in Figure 1. The

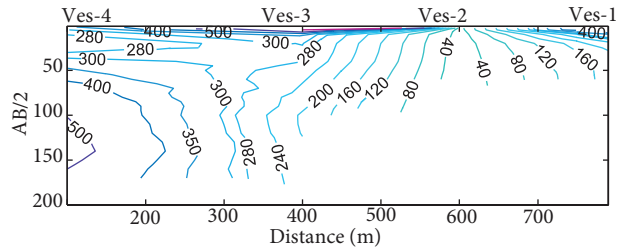


**Figure 2.** The electrical resistivity pseudo-section.

resistivity measurements were made with a METZ earth resistivity meter with stainless-steel electrodes. The maximum current electrode spacing (AB/2) was 200 m from the center of the array along the axis of the valley where surface conditions permitted. The measured apparent resistivity values were used to produce an electrical resistivity pseudo-section, which is a contour map of apparent resistivity values beneath VES-x stations at a depth proportional to their corresponding half current electrode spread (AB/2), as shown in Figure 2. The layered final geoelectric models were produced using the IPI2WIN inversion software (Bobachev *et al.* 2002). Figure 3a shows, for example, the measured apparent resistivity curve acquired at VES-3 over the ponds where warm water together with gas bubbles were observed, and Figure 3b is the geoelectric section derived from 1-D inversion. Multiple models represent the degree of equivalence in the final solution.

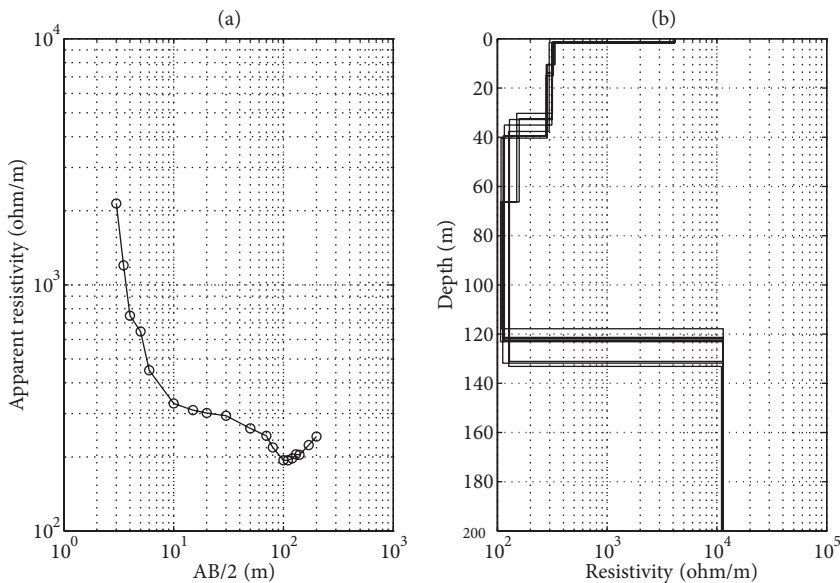


**Figure 3.** (a) VES-3 as an example of the Schlumberger resistivity sounding data and (b) equivalent (non-unique) resistivity–depth models obtained after the 1-D inversion procedure. Most models converge along the thicker black line.

Figure 4 shows the self-potential profile about 1 km long stretching along the valley axis. The measurements were carried out using a digital dc-meter connected to two CuSO<sub>4</sub> potential electrodes. Fixed electrode spacing of 20 m was maintained by moving the rear electrode to the front porous pot hole and the forward electrode to a new location. The measured gradient values were integrated to obtain the self-potential values. There are three prominent self-potential anomalies marked with roman numerals (I, II, and III) in Figure 4. The anomaly marked 'I' with 130 mV amplitude is the most prominent one measured around the pond, in which the maximum water temperature of 23 °C was measured. Similar ponds with relatively low temperatures of about 11-15 °C nicely coincide with the other two anomalies, marked II and III. Assuming the self-potential results from streaming potentials along a fault zone are as described by Murakami *et al.* (1984), we developed an inversion code in MATLAB to determine the dip angles of these faults that are expected to be related to the crack systems we identified in the field. The Table illustrates the numerical values of the model parameters estimated from each self-potential anomaly. Figure 5 illustrates the theoretical model reproduced from the initial model parameters for anomaly I, the updated model after each iteration (dotted lines), and the best-fitted fault model having a dip angle of 30°.

**4. Results and discussion**

One-dimensional geophysical measurements were carried out, since the lateral moraines at the valley sides prevented us from making geophysical measurements along directions perpendicular to the valley axis. However, the measurements produced a meaningful geophysical response since the crack system, roughly perpendicular to the valley axis, partially eliminated the shortcomings of our 1-D measurements. Figure 6 illustrates the geoelectric cross-section along with the fault model with dip angles obtained from the inversions of dc-sounding and self-potential data, respectively. The geoelectric cross-section is vertically scaled and, therefore, reflects the depth vs. resistivity values for each data set like the one presented in

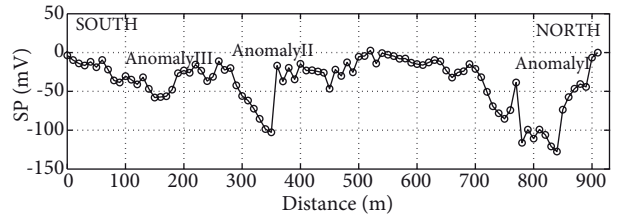


**Figure 4.** Measured self-potential profile that shows three large negative anomalies marked by roman numerals.

Figure 3b. Although the number of sounding data points is limited, the shaded low-resistivity zone is being nicely supported by the slopes of the fault models (thick solid line) that are inferred from the inversion of self-potential data. The combined results of these two independent sets of measurements suggest a crack system that dips southwards at an angle of about 30°. The low-resistivity zone shaded in Figure 6 may be interpreted to be the alteration zone that occurs at the hydrothermal fields.

The electrical resistivity pseudo-section (Figure 2) indicates an insufficient exploration depth at the VES-1 and VES-2 locations, where the chunky rock debris from the Buzulağan Valley (Figure 1) prevented placement of the electrodes any further north. A low-resistivity zone, however, is evident around VES-2. A non-unique geoelectric section produced from the inversion of vertical electrical sounding data was tested by trying a number of alternative earth models, while the fit between the observed and calculated apparent resistivity values remain similar. The example illustrated in Figure 3b indicates that there exists a conductive zone at a moderate depth represented by the heavy black line.

The MATLAB code that we developed for the inversion of the self-potential data is based on the inversion algorithm presented by Jackson (1972). Our dipping fault assumption as the source of streaming potential appears to be reasonable, since the inversion results are comparable with the geoelectric section produced using the vertical electrical sounding data (Figure 6). The inversion procedure accounts for the model parameters as being the

**Table.** Estimated values of the self-potential model parameters. The parameters  $r_1$  and  $r_2$  are the resistivity values of the either sides of the crack (fault),  $S$  is the streaming potential constant,  $a$  is the dip angle in degrees, and  $a$  and  $b$  are the depth of the top and bottom of the electrokinetic source.

Anomaly	$r_1$ (Wm)	$r_2$ (Wm)	S(mV)	$a$	$a$ (m)	$b$ (m)
I	120	150	850	30	20	100
II	100	120	750	25	15	100
III	80	100	600	36	22	95

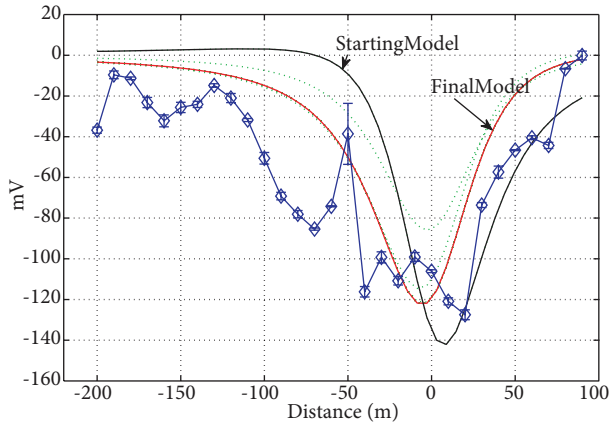


**Figure 5.** Part of the measured self-potential data (Anomaly I, diamonds) with the respective standard deviations (error bars) inverted for the fault model. The initial and the estimated values of the model parameters after the inversion are used to reproduce the theoretical data for comparison.

resistivity values on either sides of the fault, the dip angle, the depths of the top and bottom of the electrokinetic source, and the streaming potential constant. The standard deviation values of the measured self-potential data for the inversion procedure were assigned to be about 2 mV, with a few exceptions (see error bars, Figure 5). The model parameters were estimated within an acceptable range, except for the streaming constant that was estimated from its initial value because the respective eigenvalue was either too small or zero. Prediction error (or best-fit; Karaman & Carpenter 1997) exceeding 10, calculated from the anomalies, indicates noise in the self-potential measurements and also emphasizes the simplicity (or poor representation) of the fault model. The greater best-fit is also a measure of the structural complexity, as occurs with neighboring faults (or bodies) with varying slopes, etc. The inversion results presented in the Table are, however, satisfying.

The field work and the geophysical measurements indicated that the site has hydrothermal potential. This result emanated from the presence of non-freezing water ponds at the surface, the conductive zone that appears to be the alteration zone, and maximum self-potential anomalies of about 130 mV. Figure 7 illustrates a conceptual hydrothermal field with water circulation based on field observations and geophysical measurements. This circulation model explains how the hot water rises to the surface through cracks and rapidly cools on mixing with cold surface water. A test well to a depth of 60 m at the location as shown in Figure 1 (labeled “Borehole”) was drilled by an amateur team. Based on our personal communications, the presence of moderately warm water was verified from the well without cold surface water being

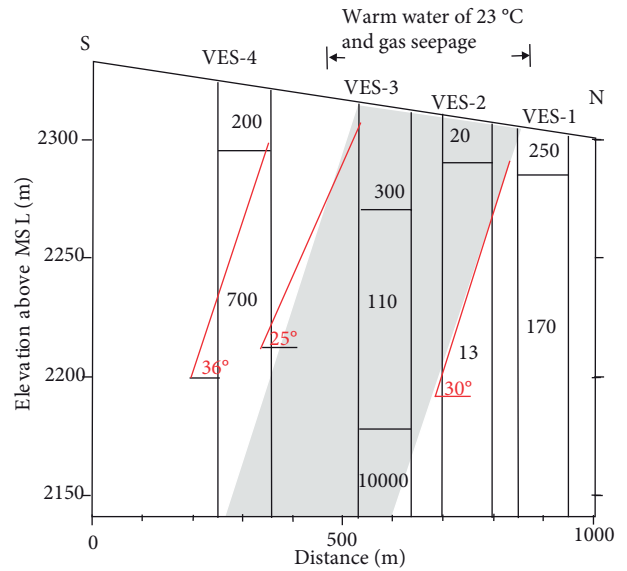


**Figure 6.** Geoelectric cross-section constructed from the interpretation of four 1-D Schlumberger vertical electrical soundings and the faults (solid lines) that are interpreted from the self-potential measurements. The numbers in the blocks are the resistivity values in ohm-meters.

fully isolated. No further test, as far as we know at the time of this work, has been carried out.

With this study, we brought up the importance of low-temperature hydrothermal fields that may lead to all-seasons investments. Even in a poor production well yield, a heat pump can be devised for local recreational centers. Although a further rigorous exploration program and drilling and production plans have to be developed for this site, the results of this simple yet effective study may produce a significant long-term impact on the future of the

A CROSS-SECTION ALONG THE ANZER GLACIAL VALLEY

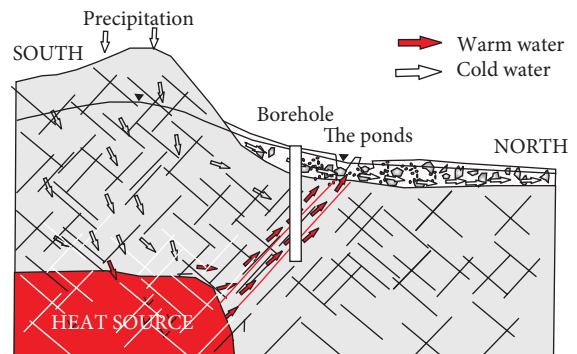


**Figure 7.** Conceptual flow model constructed from the field observations and the interpretations of the geophysical measurements. The shaded zone is where the surface water mixes with the warm water.

Eastern Black Sea region, where only limited hydrothermal site exploration has been carried out. Moreover, the minimum number of geophysical measurements produced a geoelectric cross-section that may be considered to be a unique exploration example. This study will also play a critical role to develop further exploration programs that may lead to the discovery of other potential sites in the area.

## 5. Conclusions

Low-temperature hydrothermal fields at high altitudes may stimulate investment and promote the local economy, especially in developing countries. We utilized self-potential and dc-resistivity methods in a harsh environment in the Anzer valley and acquired limited measurements only along the valley's axis. However, once a carefully studied geological target is identified, the geophysical methods prove to be very practical and useful. Based on the geophysical measurements, we were able to develop a hydrothermal water circulation model that was

verified with a test well. There are a number of conclusions that we can draw from this study that may be useful while developing future exploration programs in the region. These are: 1) site evidence, such as fungus, bacterial colonies, frogs, and insects in freezing temperatures most of the time in a year, may be a good indicator; 2) the presence of creeks and hanging valleys cutting the major valleys perpendicularly or obliquely may be related to the crack systems that play a key role for the hydrothermal circulations; and 3) utility of the dc-resistivity and self-potential methods may be a good choice for successful geophysical field work. We also conclude that the inversion of self-potential data is practical and reliable.

## Acknowledgments

This project was supported by İstanbul Technical University and Ballı Köyü Muhtarlığı. Aysun Nilay Dinç, Burak Acet Tunalı, and Enes Kılıç are thanked for their help during the field work.

## References

- Bobachev, A.A., Moudin I.N. & Shevnnin, V.A. 2002. *IPI2Win v.2.1, Resistivity Sounding Interpretation Software Package*. Moscow State University-Geoscan-M Ltd., Moscow.
- Bogoslovsky, V.A. & Ogilvy, A.A. 1973. Deformations of natural electric fields near drainage structures. *Geophysical Prospecting* **21**, 716–723.
- Corwin, R.F. & Hoover, D.B. 1979. The self-potential method in geothermal exploration. *Geophysics* **2**, 226–245.
- Doğan, A. & Kolankaya, D. 2005. Protective effect of Anzer honey against ethanol-induced increased vascular permeability in the rat stomach. *Experimental and Toxicologic Pathology* **57**, 173–178.
- Fitterman, D.V. & Corwin, R.W. 1982. Inversion of self-potential data from the Cerro Prieto geothermal field, Mexico. *Geophysics* **47**, 938–945.
- Harinarayana, T., Abdul Azeed, K.K., Murthy, D.N., Veeraswamy K., Eknath Rao, S.P., Manoj, C. & Naganjaneyulu, K. 2006. Exploration of geothermal structure in Puga geothermal field, Ladakh Himalayas, India, by magnetotelluric studies. *Journal of Applied Geophysics* **58**, 280–295.
- Harthill, N. 1978. Quadripole resistivity survey of the Imperial Valley, California. *Geophysics* **43**, 1485–1500.
- Jackson, D.D. 1972. Interpretation of inaccurate, insufficient and inconsistent data. *Geophysical Journal of the Royal Astronomical Society* **28**, 97–109.
- Karaman, A. & Carpenter, P.J. 1997. Fracture density estimates in glaciogenic deposits from P-wave velocity reductions. *Geophysics* **62**, 138–148.
- Mabey, D.R., Hoovek, D.B., O'Donnell, J.E. & Wilson, C.W. 1978. Reconnaissance geophysical studies of the geothermal system in southern Raft River Valley, Idaho. *Geophysics* **43**, 1470–1484.
- Majumdar, R.K., Majumdar, N. & Mukherjee, A.L. 2000. Geoelectric investigations in Bakreswar geothermal area, West Bengal, India. *Journal of Applied Geophysics* **45**, 187–202.
- Murakami, H., Mizutani, H. & Nebatani, S. 1984. Self-potential anomalies associated with an active fault. *Journal of Geomagnetism and Geoelectricity* **36**, 351–376.
- Ogilvy, A.A., Ayed, M.A. & Bogoslovsky, V.A. 1969. Geophysical studies of water leakage from reservoirs. *Geophysical Prospecting* **17**, 36–62.
- Okay, A.I. & Şahintürk, Ö. 1997. Geology of the Eastern Pontides. In: Robinson, A.G. (ed), *Regional and Petroleum Geology of the Black Sea and Surrounding Region*, AAPG Memoir **68**, 291–311.
- Ozkirim, A. & Keskin, N. 2001. A survey of *Nosema apis* of honey bees (*Apis mellifera* L.) producing the famous Anzer honey in Turkey. *Zeitschrift für Naturforschung C* **56**, 918–919.
- Pirajno, F. 1992. *Hydrothermal Mineral Deposits: Principles and Fundamental Concepts for the Exploration Geologist*. Springer-Verlag, Berlin.
- Reci, H., Tsokas, G.N., Papazachos, C.B., Thanassoulas, C., Avxhiou, R. & Bushati, S. 2001. Study of the cross-border geothermal field in the Sarandoporos-Konitsa area by electrical soundings. *Journal of the Balkan Society* **2**, 19–28.
- Spichak, V. & Manzella, A. 2009. Electromagnetic sounding of geothermal zones. *Journal of Applied Geophysics* **68**, 459–478.

- Storz, H., Storz, W. & Jacobs, F. 2000. Electrical resistivity tomography to investigate geological structures of the earth's upper crust. *Geophysical Prospecting* **48**, 455–471.
- Şengör, A.M.C. & Yılmaz, Y. 1981. Tethyan evolution of Turkey: a plate tectonic approach. *Tectonophysics* **75**, 181–241.
- Tripp, A.C., Ward, S.H., Sill, W.R., Swift, C.M. & Petric, W.R. 1978. Electromagnetic and Schlumberger resistivity sounding in the Roosevelt Hot Springs KGRA. *Geophysics* **43**, 1450–1469.
- Ward, S.H., Parry, W.T., Cook, W.K.L., Smith, R.B., Brown, D.F.H., Whelan, J.A., Nash, P., Sill, W.R., Chapman, S. & Bowman, J.R. 1978. A summary of the geology, geochemistry, and geophysics of the Roosevelt Hot Springs thermal area, Utah. *Geophysics* **43**, 1515–1542.
- Zohdy, A.A.R. & Bisdorf, R.J. 1990. Schlumberger soundings near Medicine Lake, California. *Geophysics* **55**, 956–964.